Anharmonic dynamics of intramolecular hydrogen bonds driven by DNA breathing

B. S. Alexandrov,[1] V. G. Stanev,[2] A. R. Bishop,[1] and K. Ø. Rasmussen[1]
[1]*Theoretical Division, Los Alamos National Laboratory, Los Alamos, New Mexico 87545, USA*
[2]*Materials Science Division, Argonne National Laboratory, Argonne, Illinois 60439, USA*
(Received 24 October 2012; published 26 December 2012)

We study the effects of the anharmonic strand-separation dynamics of double-stranded DNA on the infrared spectra of the intramolecular base-pairing hydrogen bonds. Using the extended Peyrard-Bishop-Dauxois model for the DNA breathing dynamics coupled with the Lippincott-Schroeder potential for N − H···N and N − H···O hydrogen bonding, we identify a high-frequency (∼96 THz) feature in the infrared spectra. We show that this sharp peak arises as a result of the anharmonic base-pair breathing dynamics of DNA. In addition, we study the effects of friction on the infrared spectra. For higher temperatures (∼300 K), where the anharmonicity of DNA dynamics is pronounced, the high-frequency peak is always present irrespective of the friction strength.

DOI: 10.1103/PhysRevE.86.061913 PACS number(s): 87.14.gk, 87.64.K−, 07.05.Tp, 78.30.Er

I. INTRODUCTION

The structural stability and flexibility of biomacromolecules, which play important roles in biological function [1–3], are primarily governed by hydrogen bonds (H bonds) [4]. Since the H bonds are much weaker than covalent bonds, biomacromolecules experience slow conformational motion resulting from inherent thermal fluctuations at biological temperatures. The double-stranded DNA molecule thereby experiences thermal motions that spontaneously induce large [5] openings and reclosings of the double helix (viz., "DNA breathing" [6] or "DNA bubbles" [7]). Cellular proteins exhibit similar conformational motions [8]. Many biologically important processes require such openings, which are characterized by local stretching or even disruption of intramolecular H bonds. For example, reading the genetic information encoded in DNA (transcription) or making copies of the DNA in the cell (replication) are processes that require local openings of the double helix [9,10]. Thus, the biomolecular H bonds are subject to strongly anharmonic dynamics of ubiquitous and fundamental relevance to our understanding of biological systems.

Hydrogen bonds are formed by the localized attractive interaction between a hydrogen donor and an adjacent acceptor group [see Fig. 1(a)]. One widely used tool for studying H bonds in biological macromolecules is infrared (IR) and far-infrared (FIR) spectroscopy [11]. However, at biological temperatures, the spectra are complicated by the fact that the proton motion is coupled with the stochastic intramolecular vibrations, caused by the surrounding thermal bath. Of particular importance for DNA is the localized large-amplitude breathing motion, caused by the thermal fluctuations of the surrounding water. This motion creates local openings ("bubbles") of the double helix, which leads to slow stochastic anharmonic variations of the length, $R(t)$ [Fig. 1(a)], of the H bonds between complementary base pairs and thereby affects the corresponding proton vibrations.

Because of the complexity of the problem, realistic models of biomacromolecular spectra, accounting for the surrounding water and temperature, require application of the sophisticated and numerically involved machinery of all-atoms molecular dynamics and quantum-chemical *ab initio* methods (see Ref. [11] and the works cited therein). However, to disentangle the result of such studies in the absence of a clear physical picture is challenging. Therefore, it is often desirable to consider simpler, phenomenological models, which allow some of the important issues to be addressed at much lower theoretical and computational cost. Although simplistic, such models can be useful in identifying the basic physics of biological macromolecules.

As a first step towards characterizing the effects of biomolecular breathing dynamics on H-bond IR spectra, we develop a phenomenological model of a single intramolecular H bond embedded in a short DNA molecule. We separate the H-bond system into a quantum proton subsystem and classical acceptor/donor (i.e., base pair) motion in a stochastic bath; recently, similar approaches have been used in Refs. [12,13]. To treat the proton part, we use the Lippincott-Schroeder potential [14]. This strongly anharmonic potential has been extensively used as a phenomenological model of H bonds and has shown its reliability for various molecular systems [15,16]. We couple the proton system to the strongly anharmonic breathing of a short DNA chain in a thermal environment. The DNA breathing is modeled by the nonlinear extended Peyrard-Bishop-Dauxois (EPBD) model [17,18] of DNA dynamics. The EPBD model was originally constructed to describe the stretching modes of complementary base pairs in double-stranded DNA and has been shown to be quantitatively consistent with an array of experimental observations [19].

We calculate the IR spectra of such H-bond systems, and in particular of the fundamental N − H stretching vibrations, within the framework of linear response theory, in terms of Fourier transformation of the quantum dipole time correlation function in non-Condon approximation. The derived spectra display a number of interesting features due to the strongly nonlinear nature of both subsystems. Specifically, we identify a sharp high-frequency peak and show that it arises as a result of the anharmonic base-pair breathing of DNA. We also study the effects of the friction and temperature on the spectra. In particular, we demonstrate that at high temperatures (∼300 K), where the anharmonicity of DNA breathing is pronounced, this peak is always present in the IR spectrum, irrespective of the friction strength.

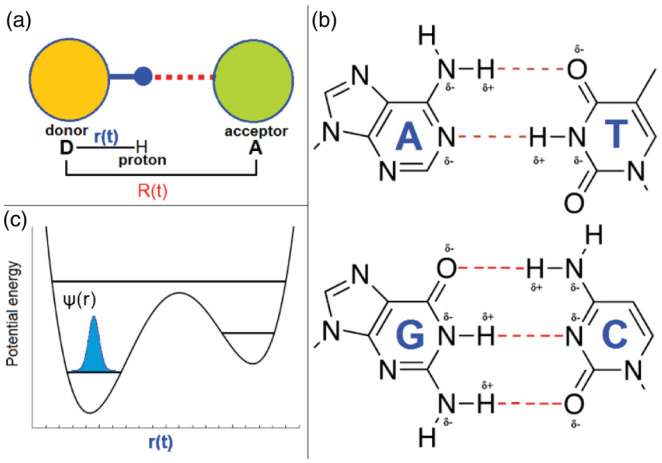

FIG. 1. (Color online) (a) Schematic representation of the donor, D, and acceptor, A. $r(t)$ is the proton and H the coordinate; $R(t)$ is the length of the hydrogen bond. (b) The intramolecular hydrogen bonds, $N-H\cdots N$, and $N-H\cdots O$, between complementary bases in the DNA molecule; adenine-thymine (AT) and guanine-cytosine (GC). (c) Illustration of the proton potential as a function of the proton coordinate r. The ground-state wave function $\psi(r)$ is illustrated in the potential.

II. MODELS AND METHODS

The intramolecular H bonds in DNA base pairs [i.e., adenine-thymine (AT), and guanine-cytosine (GC)] are of two types: $N-H\cdots N$ and $N-H\cdots O$ [see Fig. 1(b)], both of which are asymmetric. Numerous experimental and theoretical observations [20] have established that the potential-energy surface of the proton in such H bonds can be adequately represented by a double-minimum potential [see Fig. 1(c)]. This double-well structure has important consequences, such as the large polarizability of the H bond [21], which is mainly driven by the proton tunneling between the two minima. Such polarizability can be drastically influenced by the presence of even a small external field (the effect is strongest for symmetric potentials, but it is also present for asymmetric potentials) and can be orders of magnitude larger than in systems (e.g., free water) where the main contribution is due to electrons [22]. Therefore, the direct influence of the external field on the electrons can reasonably be neglected in the treatment of biomolecular H bonds.

As discussed above, at biological temperatures, an important feature of the intramolecular DNA dynamics is the localized large-amplitude breathing motion, caused by the thermal fluctuations. At these temperatures the dynamics of the H bonds between complementary bases [Fig. 1(c)] can be qualitatively understood as a result of the anharmonic coupling of two distinct [fast (quantum) and slow (classical)] modes. To treat this coupling, we utilize the Born-Oppenheimer approximation, in which the slow mode is represented as a classical and stochastic vibrational displacement of the acceptor-donor pair, i.e., the transverse stretching of the hydrogen bond. This slow mode is coupled to the fast and intrinsically quantum mode, associated with the motion of the proton in the potential created by the two nucleotides forming the DNA base pair.

For a single (quasi-one-dimensional) hydrogen bond, the proton Hamiltonian is

$$\hat{H}_{\text{proton}} = -\frac{\hbar^2}{2m_p}\frac{\partial^2}{\partial r^2} + V(r,R). \tag{1}$$

At biological thermal and solvation conditions, the length of the H bond R is a parameter in $\hat{H}_{\text{proton}}$. Due to the large masses of the nucleotides and their slow conformational motion, this problem is well posed within the Born-Oppenheimer approximation, and the back-reaction of the quantum motion on the classical vibration can be neglected. The proton couples to the classic motion due to changes in the base-pair displacement, which modulates the shape of $V(r,R)$. For the proton potential we use the strongly nonlinear Lippincott-Schroeder (LS) potential [14]

$$V_{\text{LS}}(r,R) = V_1(r) + V_2(r,R) + V_3(R) + V_4(R). \tag{2}$$

Here, V_1 represents the donor-proton interaction and V_2 the proton-acceptor interaction, and V_3 and V_4 represent the repulsive and attractive interactions between the donor and acceptor groups and are functions only of the acceptor-donor distance, $R(t)$. These potentials have the form

$$V_1 = D\left[1 - e^{-\frac{\nu}{2r}(r-r_0)^2}\right], \tag{3}$$

$$V_2 = D^*\left[1 - e^{-\frac{\nu^*}{2(R-r)}(R-r-r_0^*)^2}\right] - D^*, \tag{4}$$

$$V_3 = Ae^{-bR}, \tag{5}$$

$$V_4 = -B/R^m. \tag{6}$$

In Eqs. (3)–(6) D and r_0 are the dissociation energy and equilibrium distance of the donor-proton bond, respectively; D^* and r_0^* are similar parameters for the proton-acceptor bond. The parameter $\nu = \kappa r_0/D$, where κ is the force constant for the stretching vibration of the non-hydrogen-bonded donor-proton group; similarly, $\nu^* = \kappa^* r_0^*/D^*$. The parameters A and B can be determined at the equilibrium base-pair distance R_0 (for estimates, see, for example, Ref. [23]), at which we require $(\partial V_{\text{LS}}/\partial R) = 0$. This condition has to be evaluated at the equilibrium proton position r, determined from $(\partial V_{\text{LS}}/\partial r) = 0$ (for details see Ref. [14]). The numerical values of the parameters are given in Ref. [24].

Note that the use of the LS potential is not formally justified for the specificity of the DNA intramolecular H bonds, since this potential has primarily been designed and optimized for bonds in much simpler molecules (e.g., water molecules). Detailed comparison with quantum chemistry computations, however, show that LS is a reasonable approximation for the GC base pair [25]. Here, we are using the parameters justified for GC base pair, as well as for AT base pairs, assuming that the LS potential retains the most important qualitative features present in the microscopic calculations and it will provide at least qualitative insight into the problem. In the case of $N-H\cdots O$ bonds, there is the additional complication that the NH stretching of the H bond is coupled to the NH_2 stretching vibration [26], which makes it intrinsically two dimensional. For that reason, we concentrate on the $N-H\cdots N$ mode.

For the H-bond length, $R(t)$, we have $R(t) = R_0 + y_n(t)$, where R_0 is the equilibrium distance between two complementary nucleotides and $y_n(t)$ is the stochastic change of this length (at the nth base pair) caused by the solvent. The stochastic behavior of $y_n(t)$ at room temperature is often modeled as a classical Ornstein-Uhlenbeck process that satisfies a harmonic Langevin equation [27]. Here we will use instead the stochastically driven EPBD model [18,28] of double-stranded DNA in order to capture the nonlinear behavior of the DNA breathing,

$$m\ddot{y}_n = -U'(y_n) - W'(y_{n+1}, y_n) - W'(y_n, y_{n-1}) - m\gamma\dot{y}_n + \eta(n,t), \tag{7}$$

where

$$U(y_n) = D_n[\exp(-a_n y_n) - 1]^2 \tag{8}$$

represents the hydrogen bonding of the complementary bases and

$$W(y_n, y_{n-1}) = \frac{k_{n,n-1}}{2}\left[1 + \rho e^{-\beta(y_n + y_{n-1})}\right](y_n - y_{n-1})^2 \tag{9}$$

represents the stacking energy between consecutive base pairs. γ and $\eta(n,t)$ are the drag and stochastic drive of the solvent and obey the standard fluctuation-dissipation relationship. The parameters D_n, a_n depend on the type of base pair (AT or GC) [17]. The dinucleotide stacking force constants $k_{n,n-1}$ depend on the nature of the consecutive nucleotides $(n,n-1)$ [18]. The values $\beta = 0.35$ and $\rho = 2$ were determined based on DNA melting experiments [29]. It is noteworthy that the base pairs in a poly(G) sequence (containing only guanine bases in the 5′ to 3′ strand) open significantly less than the base pairs of a poly(A) sequence (containing only adenine bases in the 5′ to 3′ strand). Another important feature of the distribution of $R(t)$ is the long and slowly decaying tail, suggesting the existence of large bubble openings in the sequence [the tail is more pronounced for poly(A)].

We treat the anharmonic coupling between the fast quantum and the slow classical modes in several steps. First, we numerically solve the Schrödinger equation with the LS potential for a broad range of values of R and obtain the energy levels and the eigenstates of the proton. Specifically, we solve the Schrödinger equation with the LS potential by direct diagonalization for each value of R. To illustrate the results, we show in Fig. 2 the energetic difference, $\omega_{01}(R)$, between the proton ground state and the first excited state as a function of R. Note that due to the strong anharmonic character of the LS potential, $\omega_{01}(R)$ has a rather nontrivial behavior. For $R > 3.5$ Å $\omega_{01}(R)$ saturates at about 96 THz. This saturation reflects the fact that for larger openings (viz., local disruption of the H bond) the LS potential has two distinct and well-separated wells, and tunneling between these states is practically impossible. Note that a similar effect should be present for all realistic H-bond potentials that take into account the DNA breathing, i.e., the local disruption of H bonds. Next, from the classical (slow) time dependence of the $R(t)$ we have the time dependence of the dipole moment operator $\hat{\mu}(R)$ and the time dependence of the energy levels $\omega_{0k}(R)$. We calculate the time dependence of the dipole moment matrix elements, $\mu_{0k}(t)$, and the dipole-dipole autocorrelation function

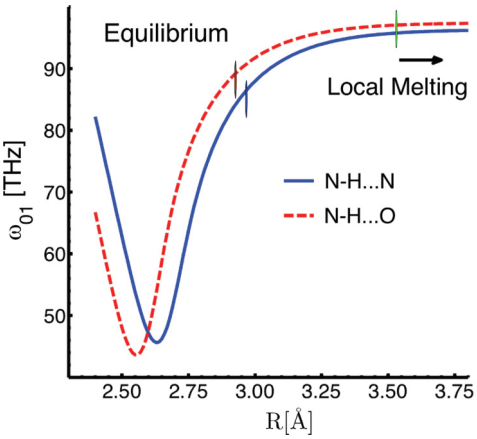

FIG. 2. (Color online) The energy difference $\omega_{01} = (E_1 - E_0)/\hbar$ between the ground state E_0 and the first excited state E_1 (E_0 and E_1 are the first eigenvalues of $\hat{H}_{\text{proton}}$) versus base-pair separation, R, of the N − H···N [solid (blue) line] and N − H···O [dashed (red) line] H bonds, as modeled by the Lippincott-Schroeder potential.

$$\langle\mu(0)\mu(t)\rangle = \sum_k \left\langle |\mu_{k0}(0)|^2 e^{-i\int_0^t d\tau\omega_{0k}(\tau))}\right\rangle, \tag{10}$$

whose Fourier transform

$$I(\omega) = \frac{1}{2\pi}\int_{-\infty}^{\infty} dt e^{-i\omega t}\langle\mu(0)\mu(t)\rangle \tag{11}$$

is related to the IR absorption coefficient

$$\alpha(\omega) = \frac{4\pi^2\omega}{3V\hbar c n_{\text{ref}}(\omega)}(1 - e^{-\beta\hbar\omega})I(\omega). \tag{12}$$

Here V is the system volume, $n_{\text{ref}}(\omega)$ the refractive index at frequency ω, c is the speed of light, and $\beta = 1/k_B T$, with k_B the Boltzmann constant and T the temperature.

III. RESULTS AND DISCUSSION

There are two distinct limits of the time dependence of the dipole moment autocorrelation function [Eq. (10)] that can be discussed separately. In the limit of large friction the classical system becomes overdamped and the stochastic averaging in Eq. (10) can be performed by using the probability distribution, $P(R)$, for the classical variable, $R(t)$. This statistical approach was pioneered by Bratož *et al.* [30] (see also Ref. [31]). In this limit the dipole-dipole autocorrelation function simplifies to

$$\langle\mu(0)\mu(t)\rangle = \sum_k \int_0^{\infty} P(R)\mu_{0k}^2(R)e^{-i\omega_{0k}(R)t}dR. \tag{13}$$

Generally, in this limit we expect the spectrum to consist of peaks associated with the proton transitions at the most probable $R = R_m$, broadened by the variation of the transition frequencies $\omega_{0k}(R(t))$ with R (through its distribution function). In the opposite limit of low friction the classical system is underdamped and we can think of the system as two coupled strongly anharmonic oscillators (dynamical approach) [27]. In this case the frequency $\omega_{01}(R(t))$, although with a stochastic nature, demonstrates certain periodicity in time, and we expect the coupling to produce satellite peaks,

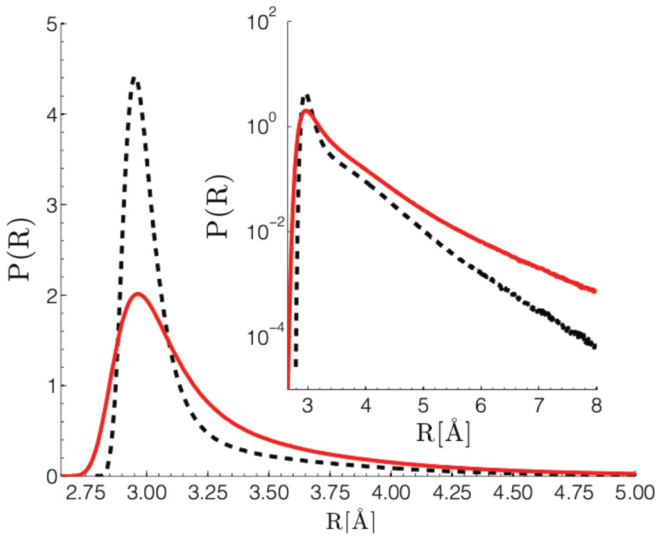

FIG. 3. (Color online) Equilibrium distributions $P(R)$ of the base-pair separation, R $[R(t) = R_0 + y_n(t)]$, at $T = 300$ K for poly(A) [solid (red) line] and poly(G) [dashed (black) line] sequences as generated by 1-μs EPBD Langevin dynamics. In order to highlight the long tails of the distributions the inset shows the same distributions in a semilogaritmic scale.

shifted by the frequency of the classical slow motion: Ω, of the main proton transitions (see Ref. [27], which presents an extensive discussion of the relevant energy/time scales and gives precise definitions of the limits of "low" and "high" friction).

We begin with the high friction limit that will provide us with important insights into the general problem. For simplicity, we will, from now on, only consider transitions to the first excited state ($n = 1$). In order to obtain the equilibrium distributions $P(R)$, we performed Langevin dynamics simulations of the EPBD model. Specifically, we generated 1000 independent trajectories, each of 1-ns duration, which subsequently are binned at 1-fs resolution to create $P(R)$. Figure 3 shows the distributions for poly(A) and poly(G) sequences, respectively. We can now use these distributions in the described statistical approach formalism, Eq. (13). The resulting IR spectra are shown in Fig. 4. In Fig. 4(a) the spectra for both poly(A) and poly(G) at low temperature ($T = 77$ K) are shown. The central peak is due to the proton transition from the ground state to the first excited state, and the broadening results from the thermal fluctuations of the classical coordinate, $R(t)$. The differences in broadening and the peak maximum position for the two sequences can be traced to the different features in the probability distribution of $P(R)$. The inset in Fig. 4(a) shows the room-temperature spectra for the same sequences. We can see that the shape of the IR absorption has changed dramatically as a result of the increase of temperature. The low-temperature peak has been reduced [for poly(G)] and completely smeared [for poly(A)], while a new sharp peak has emerged at higher frequencies. The appearance of such a sharp feature at *high* temperatures at first seems puzzling but is, in fact, a natural consequence of the strong anharmonicity of both the classical and quantum subsystems. At room temperatures, because of its nonlinearity, we expect the EPBD model to produce a significant density of

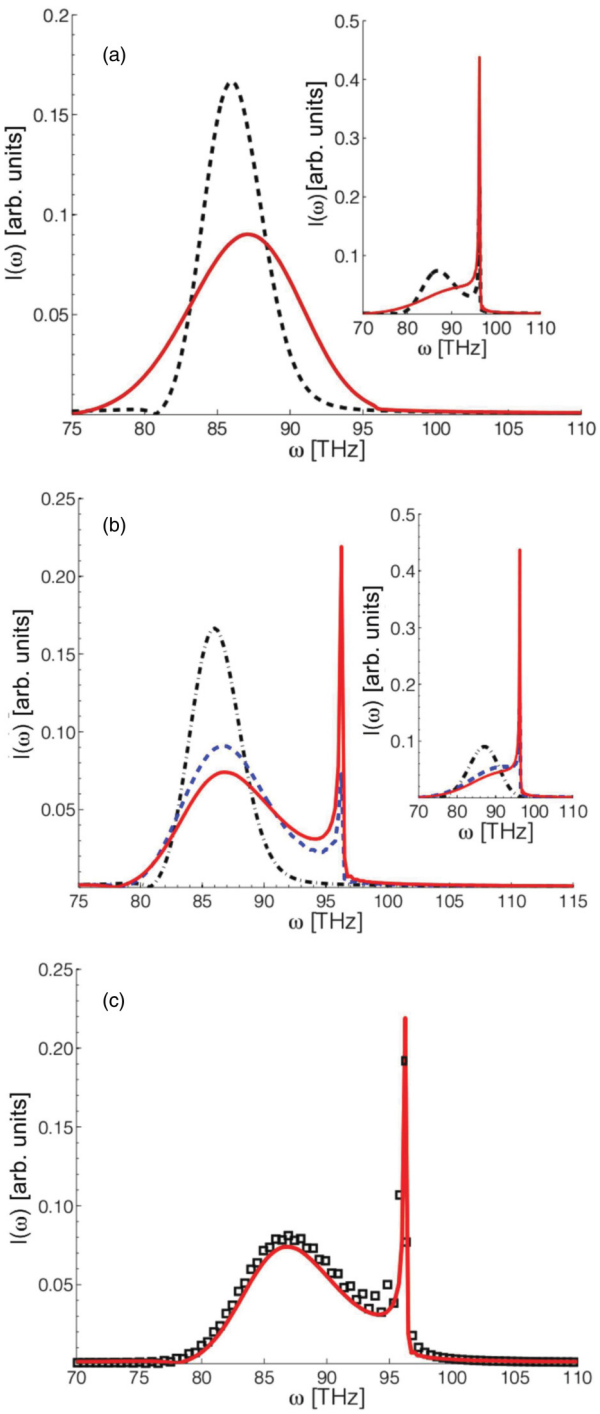

FIG. 4. (Color online) IR spectra of a N-H..N bond calculated by the statistical approach, Eq. (13). A) Low temperature $T = 77K$ spectra for poly(A) (solid (red) line) and poly(G) (dashed (black) line) sequences. Inset shows the spectra at $T = 300K$. B) Temperature dependence of poly(G) spectra. Dash-dotted (black) line shows $T = 77K$, dashed (blue) line $T = 280K$, and solid (red) line $T = 300K$. Inset shows the temperature dependence of poly(A) sequence. C) Comparison of results from statistical approach (solid (red) line) and dynamical approach (black squares) derived in high friction limits, $\gamma = 2000ps^{-1}$.

bubble states representing the breathing dynamics of the DNA molecule. This leads to an extended tail in the distribution $P(R)$ (Fig. 3). As already explained, however, all the states

with $R > 3.5$ Å results in a frequency response around 96 THz, and this bubble density of states produces the new sharp peak. Hence, the larger and more frequent the bubbles are, the more intense is this peak. Note that as the temperature increases the most probable value R_m also increases, producing a blue shift of the peak, associated with proton transitions for R_m. As a result of this shift, the two peaks essentially merge in the poly(A) case and produce a single, intense, and sharp peak, with a broad shoulder on the low-frequency side. In the case of poly(G) the two features are still well separated and about equal in intensity. We can also follow the temperature dependence of the high-frequency peak for the poly(G) [shown in Fig. 4(b)]. Note how it appears and grows *without* moving in energy or changing its width, which is consistent with our interpretation. The low-temperature peak, in contrast, undergoes a (small) blue shift and also becomes broader, as expected.

Now we turn to the dynamical approach. We treat it by using the EPBD model to numerically generate representative trajectories for $R(t)$ and use these to calculate $I(\omega)$. First, we compare results from the dynamical approach derived in the limit of high friction with that obtained by the statistical approach. We see that the two calculations give essentially identical results [Fig. 4(c)]. Turning to the case of low friction, $\gamma = 0.05\ \mathrm{ps}^{-1}$, we expect the classical frequency Ω to enter the spectrum of the quantum system producing additional peaks in the vicinity of the peaks ascribed to the proton transitions at the most probable R. At low temperatures, in the case of a poly(G) sequence, we see one central sharp peak, accompanied by two much weaker peaks at roughly $\omega \pm \Omega$, where ω/Ω is the quantum (classical) frequency [Fig. 5(a)]. Similar structures have been observed in previous calculations, even for the much simpler case of coupled harmonic oscillators [27,32]. The case of the poly(A) sequence differents markedly [Fig. 5(b)]. Here we observe several peaks, at approximately $\omega \pm \frac{n}{2}\Omega$, where n is an integer. The occurrence of subharmonics in the classical system and the fact that the intensity of several of the central peaks is comparable is a clear signature of the strongly anharmonic dynamics of the poly(A) sequence. With increasing temperature, the respective structures survive (albeit broader and less intense) but are again dwarfed by a peak around 96 THz at room temperatures [Fig. 5(b)]. Its origin is exactly the same as in the case of large friction—the huge density of bubble states corresponding to this frequency, which become increasingly pronounced with the temperature.

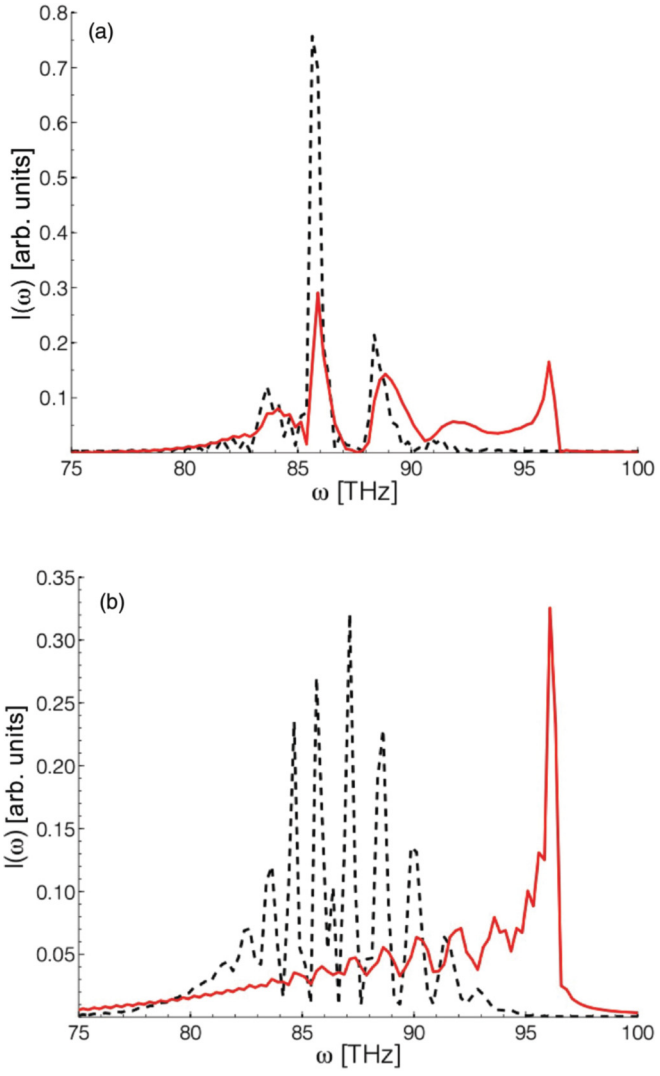

FIG. 5. (Color online) IR spectra of a N − H···N bond calculated by the dynamical approach in the low friction limit $\gamma = 0.05\ \mathrm{ps}^{-1}$. (a) Poly(G) sequence for $T = 77$ K [dashed (black) line] and $T = 300$ K [solid (red) line]. (b) Poly(A) sequence for $T = 77$ K [dashed (black) line] and $T = 300$ K [solid (red) line].

IV. CONCLUSION

We have reported effects of the anharmonic strand-separation dynamics of double-stranded DNA on the infrared spectra of the intramolecular base-pairing H bonds. We have used the well-established EPBD model to characterize anharmonic dynamics of DNA sequences. This dynamics was coupled to Lippincott-Schroeder potentials for N − H···N and N − H···O H bonds and linear response calculations were performed to determine infrared spectra. A new high-frequency feature at about 96 THz was identified to arise as a direct result of the anharmonic breathing dynamics, i.e., as a result of the already-observed [6,7] base flipping (H-bond disruption) from the DNA stack. We show that this feature dominates the NH line in bulk water irrespective of the dissipation environment, at least at high temperatures (∼300 K), where the DNA dynamics is highly anharmonic and should not be very sensitive to the particulars of the H-bond models that can take into account local and temporal disruption of the H bond. While experimental observations of this novel spectral feature may be hampered by absence of bulk water, or by spectral interference from infrared signatures arising from the solvent, e.g., from OH stretching absorption of surrounding water and from NH_2 stretching absorption as well from the absorption of the H bonds of the rest of the base pairs in the sequence, its existence could present an intriguing new path to quantify and characterize the anharmonic dynamics of double-stranded DNA. In particular, the observation and detailed experimental interrogation of this feature may lead to an efficient submillimeter molecular spectroscopy method for the study of low-frequency nonlinear dynamical properties of nucleic acids and even of other complex biological

molecules. As it has becoming increasingly clear that large-amplitude motions of biological molecules play a significant role in important biological processes such as transcription and protein-DNA interactions [19] experimental methods to characterize and even control [33] these motions will become increasingly important.

ACKNOWLEDGMENTS

This research was carried out under the auspices of the National Nuclear Security Administration of the US Department of Energy at Los Alamos National Laboratory under Contract No. DE-AC52-06NA25396.

[1] Edited by T. Ohyama, *DNA Conformation and Transcription*, 1st ed. (Springer, Berlin, 2005).

[2] A. R. Bishop, K. Ø. Rasmussen, A. Usheva, and B. S. Alexandrov, in *Entropy–Driven Conformations Controlling DNA Functions*, Springer Series in Materials Science, Vol. 148, edited by T. Kakeshita, T. Fukuda, N. S. Saxena, and A. Planes (Springer, Berlin, Heidelberg, 2012).

[3] S. Damjanovich, B. Somogyi, and G. R. Welch. J. Theor. Biol. **105**, 25 (1983); J. Bhalla, G. B. Storchan, C. M. MacCarthy, V. N. Uversky, and O. Tcherkasskaya, Mol. Cell. Proteom. **5**, 1212 (2006); S. Tripathi and J. J. Portman, J. Chem. Phys. **135**, 075104 (2011).

[4] G. L. Pimentel and A. L. McClellan, *The Hydrogen Bond* (W. H. Freeman, San Francisco, CA, 1960).

[5] P. R. von Hippel and K.-Yi. Wong, J. Mol. Biol. **61**, 587 (1971).

[6] M. Gueron, M. Kochoyan, and J. L. Leroy, Nature **328**, 89 (1987).

[7] S. W. Englander, N. R. Kallenbach, A. J. Heeger, J. A. Krumhansl, and S. Litwin, Proc. Natl. Acad. Sci. USA **77**, 7222 (1980).

[8] S. W. Englander, D. B. Calhoun, J. J. Englander, N. R. Kallenbach, R. K. H. Liem, E. L. Malin, C. Mandal, and J. R. Rogero, Biophys J. **32**, 577 (1980).

[9] K. Skarstad, T. A. Baker, and A. Kornberg, The EMBO J. **9**, 2341 (1990).

[10] U. Siebenlist, Nature **279**, 651 (1979).

[11] Edited by T. Elsaesser and H. J. Bakker, *Ultrafast Hydrogen Bonding Dynamics and Proton Transfer Processes in the Condensed Phase* (Springer, Berlin, 2010).

[12] S. Roy, J. Lessing, G. Meisl, Z. Ganim, A. Tokmakoff, J. Knoester, and T. L. C. Jansen, J. Chem. Phys. **135**, 234507 (2011).

[13] Tatsuya Joutsukaa and Koji Ando, J. Chem. Phys. **134**, 204511 (2011).

[14] E. R. Lippincott and R. Schroeder, J. Phys. Chem. **23**, 1099 (1955); **61**, 921 (1957).

[15] M. V. Vener, Chem. Phys. Lett. **244**, 89 (1995).

[16] F. Perakis, S. Widmer, and P. Hamm, J. Chem. Phys. **134**, 204505 (2011).

[17] M. Peyrard and A. R. Bishop, Phys. Rev. Lett. **62**, 2755 (1989); T. Dauxois, M. Peyrard, and A. R. Bishop, Phys. Rev. E **47**, R44 (1993).

[18] B. S. Alexandrov, V. Gelev, Y. Monisova, L. B. Alexandrov, A. R. Bishop, K. Ø. Rasmussen, and A. Usheva, Nucl. Acids Res. **37**, 2405 (2009).

[19] B. S. Alexandrov, K. Ø. Rasmussen, and A. R. Bishop, J. Biol Phys. **35**, 31 (2009).

[20] G. Zundel, in *Advances in Chemical Physics*, Vol. 111, edited by I. Prigogine and S. A. Rice (John Wiley & Sons, Inc., Hoboken, NJ, USA, 2007).

[21] R. Janoschek, E. G. Weidemann, H. Pfeiffer, and G. Zundel, J. Am. Chem. Soc. **94**, 2387 (1972).

[22] E. G. Weidemann and G. Zundel, Z. Naturforsch. Teil A **25**, 627 (1970).

[23] J. M. Rosenberg, N. C. Seeman, R. O. Day *et al.*, Biochem. Biophys. Res. Commun. **69**, 979 (1976).

[24] For the $N-H\cdots N$ bond we use parameter values $D = 104$ kcal/mol, $n = 9.30$ Å^{-1}, $n^* = 13.49$ Å^{-1}, $r_0 = 1.014$ Å, $r_0^* = 1.014$ Å, $b = 4.8$ Å, $m = 1$, with equilibrium proton position $r = 1.0358$ Å and equilibrium $N-N$ distance $R_0 = 2.95$ Å; for the linear $N-H\cdots O$ bond we use parameter values $D = 104$ kcal/mol, $n = 9.30$ Å^{-1}, $n^* = 13.15$ Å^{-1}, $r_0 = 0.99$ Å, $r_0^* = 0.96$ Å, $b = 4.8$ Å, $m = 1$, with equilibrium proton position $r = 1.0366$ Å, $R_0 = 2.91$ Å [14].

[25] D. K. Ray and J. Ladik, J. Mol. Spec. **27**, 79 (1968).

[26] M. Yang, L. Szyc, and T. Elsaesser, J. Phys. Chem. B **115**, 13093 (2011).

[27] J. Yarwood and G. N. Robertson, Nature **257**, 41 (1975); G. N. Robertson and J. Yarwood, Chem. Phys. **32**, 267 (1978).

[28] B. S. Alexandrov, L. T. Wille, K. Ø. Rasmussen, A. R. Bishop, and K. B. Blagoev, Phys. Rev. E **74**, 050901(R) (2006).

[29] A. Campa and A. Giansanti, Phys. Rev. E **58**, 3585 (1998).

[30] S. Bratož, J. Rios, and Y. Guissani, J. Phys. Chem. **52**, 439 (1970); S. Bratož, J. Chem. Phys. **63**, 3499 (1975).

[31] H. Romanowski and L. Sobczyk, Chem. Phys. **19**, 361 (1977).

[32] W. G. Johnson and D. W. Oxtoby, J. Chem. Phys. **87**, 781 (1987).

[33] J. Bock, Y. Fukuyo, S. Kang, M. L. Phipps, L. B. Alexandrov, K. Ø. Rasmussen, A. R. Bishop, E. D. Rosen, J. S. Martinez, H.-T. Chen, G. Rodriguez, B. S. Alexandrov, and A. Usheva, PLoS ONE **5**, e15806 (2010).